

Submitted to Astrophysical Journal Letters

Meridional Transport in the Stratosphere of Jupiter

Mao-Chang Liang^{1*}, Run-Lie Shia¹, Anthony Y.-T. Lee¹, Mark Allen^{1,2}, A. James Friedson², and Yuk L. Yung¹

¹*Division of Geological and Planetary Sciences, California Institute of Technology, Pasadena, CA 91125*

²*Jet Propulsion Laboratory, California Institute of Technology, Pasadena, CA 91109*

*To whom all correspondence should be addressed. E-mail:
mcl@gps.caltech.edu

ABSTRACT

The Cassini measurements of C_2H_2 and C_2H_6 at ~ 5 mbar provide a constraint on meridional transport in the stratosphere of Jupiter. We performed a two-dimensional photochemical calculation coupled with mass transport due to vertical and meridional mixing. The modeled profile of C_2H_2 at latitudes less than 70° follows the latitude dependence of the solar insolation, while that of C_2H_6 shows little latitude dependence, consistent with the measurements. In general, our model study suggests that the meridional transport timescale above 5-10 mbar altitude level is $\gtrsim 1000$ years and the time could be as short as 10 years below 10 mbar level, in order to fit the Cassini measurements. The derived meridional transport timescale above the 5 mbar level is a hundred times longer than that obtained from the spreading of gas-phase molecules deposited after the impact of Shoemaker-Levy 9 comet. There is no explanation at this time for this discrepancy.

Subject headings: planetary systems—radiative transfer—atmospheric effects—planets and satellites: individual (Jupiter)—methods: numerical

1. Introduction

Meridional advection and mixing processes in the atmosphere of Jupiter are poorly known. Based on the Voyager infrared spectrometer data, several efforts to derive the atmospheric circulation have been published (e.g., Gierasch et al. 1986; Conrath et al. 1990;

West et al. 1992). The first direct and quantitative derivation of meridional transport processes is based on the introduction of aerosol debris into the atmosphere of Jupiter by comet Shoemaker-Levy 9 (SL9). Friedson et al. (1999) conclude that the advection by the residual circulation calculated by West et al. (1992) is insufficient to explain the temporal distribution of cometary debris. Meridional eddy mixing coefficients on the order of $1\text{--}10 \times 10^{10} \text{ cm}^2 \text{ s}^{-1}$ are inferred in the regions between ~ 10 and 100 mbar. Later, based on the time evolution profiles of CO, CO₂, CS, HCN, and H₂O gas-phase molecules deposited after the SL9 impact, values of meridional eddy mixing coefficients as high as $2\text{--}5 \times 10^{11} \text{ cm}^2 \text{ s}^{-1}$ are derived for pressures between $\sim 0.1\text{--}0.5$ mbar (Lellouch et al. 2002; Moreno et al. 2003; Griffith et al. 2004).

The Cassini measurements of stratospheric C₂H₂ and C₂H₆ (Kunde et al. 2004) provide good tracers for characterizing mass transport in the upper atmosphere of Jupiter. However, the weighting function of these observations is such that they are most sensitive to the altitude level near 5 mbar. Kunde et al. show that, at latitudes equatorward of $\sim 70^\circ$, the relative magnitude of the abundance (or emission line intensity) of C₂H₂ follows the latitudinal variation in solar insolation, while the abundance (or emission line intensity) of C₂H₆ is constant with latitude. Consequently, Kunde et al. conclude that the stratospheric meridional transport timescale at latitudes $< 70^\circ$ derived from these Cassini data falls between the lifetimes of C₂H₂ and C₂H₆. Due to the complexity in the auroral regions (contamination of line emissions from higher atmosphere due to temperature enhancement), we focus on the regions with latitude less than $\sim 70^\circ$ in this paper.

2. Two-Dimensional Transport Model

Because of the rapid rotation of Jupiter and its strong stratospheric zonal wind, the zonal variations in abundances should be minimized¹. Therefore, a two-dimensional (2-D) model including net meridional and vertical transport should be an adequate first-order simulation of these Cassini observations of the trace hydrocarbon species. In the 2-D mode, the Caltech/JPL coupled chemistry/transport code, solves the mass continuity equation:

$$\frac{\partial n_i(y, z, t)}{\partial t} + \nabla \cdot \vec{\varphi}_i(y, z, t) = P_i(y, z, t) - L_i(y, z, t), \quad (1)$$

where n_i is the number density for the species i , φ_i the transport flux, P_i the chemical production rate, and L_i the chemical loss rate, all evaluated at time t , latitudinal distance

¹The rotation period and atmosphere-radiative timescale is ~ 10 hours and ~ 1000 days (at ~ 10 mbar) (Flasar 1989), respectively.

y and altitude z . Reported herein are results for diurnally averaged steady-state solutions, i.e., $\langle \partial n_i / \partial t \rangle \rightarrow 0$.

For one-dimensional (1-D) problems (y dependence in eqn.(1) vanishes), the Caltech/JPL code (see, e.g., Gladstone et al. 1996) integrates the continuity equation including chemistry and vertical diffusion for each species using a matrix inversion method that allows large time steps. To take advantage of the computational efficiency of the 1-D solver, a “quasi 2-D” mode, which is a series of 1-D models at different latitudes coupled by meridional transport, has been developed. This quasi 2-D simulation has been tested against a case which has a known solution (Shia et al. 1990). Since the meridional transport in the stratosphere is not well understood, the quasi 2-D model uses a simple parameterization for mixing between the neighboring 1-D columns to simulate the meridional transport, i.e., $K_{yy} \partial n_i / \partial y$ is added to the results of the 1-D computations, where K_{yy} is the meridional mixing coefficient. Our work provides an order of magnitude estimate of the meridional transport in the stratosphere.

The vertical mixing coefficients (K_{zz}) and temperature profile are taken from Gladstone et al. (1996) and are assumed to be independent of latitude in the reference model. Sensitivities of the results due to the variations of temperature and K_{zz} profiles are also presented.

The meridional mixing K_{yy} will be determined by fitting the Cassini measurements (Kunde et al. 2004). As a first order approximation, the K_{yy} profile will be assumed also to be latitude-independent.

The model atmosphere is gridded latitudinally and vertically in 10 and 131 layers, respectively. The vertical grid size is chosen to insure that there are >3 grid points in one pressure scale height (to achieve good numerical accuracy). The latitude grid points are at 10, 30, 50, 70, and 85° in each hemisphere.

The photochemical reactions (P_i and L_i) are taken from Moses et al. (2000). At all latitudes, the mixing ratio of CH_4 in the deep atmosphere is prescribed to be 2.2×10^{-3} , and the atomic hydrogen influx from the top atmosphere is fixed at $4 \times 10^9 \text{ cm}^{-2} \text{ s}^{-1}$ (see, e.g., Gladstone et al. 1996). In order to prevent the solution from oscillating seasonally, the inclination angle of Jupiter is prescribed to be zero ($\sim 3^\circ$ actually).

3. Simulation Results

The Cassini measurements of the latitudinal distribution of C_2H_2 and C_2H_6 are reproduced in Fig. 1; the contribution function for these is near 5 mbar (Kunde et al. 2004).

Since the absolute abundances of C_2H_2 and C_2H_6 have not been determined from these measurements, the results shown are arbitrarily scaled following the approach of Kunde et al. Because the C_2H_2 abundances follow the latitudinal distribution of insolation (insolation is proportional to cosine of latitude), the meridional mixing timescale is expected to be longer than the C_2H_2 photochemical lifetime. On the other hand, since the C_2H_6 abundance appears to be constant with latitude, the meridional mixing timescale is expected to be shorter than the C_2H_6 photochemical lifetime.

A more quantitative estimate for K_{yy} can be derived from the 2-D model. A validation of the 2-D model is from a 1-D model for Jovian hydrocarbon chemistry (Gladstone et al. 1996; Moses et al. 2005), which reproduces extensive observations of hydrocarbon species as well as He 584 Å and H Lyman- α airglow emissions at low latitudes (observations are summarized in the Tables 1 and 5 of Gladstone et al. 1996 and Fig. 14 of Moses et al. 2005). The chemical loss timescales for C_2H_2 and C_2H_6 drawn from our current work are shown in Fig. 2, along with vertical mixing timescales (also from our current work). At 5 mbar, the chemical loss timescales for C_2H_2 and C_2H_6 are about 10 and 2000 years, respectively. Therefore, to reproduce the Cassini distributions of C_2H_2 and C_2H_6 , the meridional mixing time must fall within 10 and 2000 years at 5 mbar.

Many simulations were performed with the quasi-2D model to explore the sensitivities of the abundances C_2H_2 and C_2H_6 at 5 mbar to the choice of K_{yy} . The results were parameterized in terms of the ratio of the abundance at 70° latitude to the abundance at 10°. In general, the altitude variation of K_{yy} leading to a latitudinal gradient for C_2H_2 consistent with the Cassini observations also led to a sharp reduction in the C_2H_6 abundance from equator to near-pole. Alternatively, for many cases tested, if the C_2H_6 equator to near-pole variation was small, the same was true for the C_2H_2 equator to near-pole variation. Shown in Table 1 are the model results that most adequately reproduce the Cassini observations. We found that a ‘transition’ level somewhere around 5 and 10 mbar must be present, in order to match the Cassini measurements. Above the transition altitude, $K_{yy} \lesssim 10^9 \text{ cm}^2 \text{ s}^{-1}$. Below the transition altitude, $K_{yy} > 2 \times 10^{10} \text{ cm}^2 \text{ s}^{-1}$, consistent with the analysis of the temporal spreading of the SL9 debris (Friedson et al. 1999). It is interesting to note that the results of Friedson et al. predict a reversal in the direction of the meridional component of the annual-mean residual velocity across the 5 mbar level in the southern hemisphere. This reversal represents a change with altitude in the relative contributions to the total annual-mean meridional heat flux from the component associated with the Eulerian-mean meridional velocity and the component associated with eddies. It is therefore possible that a change in the efficiency of meridional transport accompanies the reversal.

These model results can be understood in the context of the basic photochemistry

controlling the production and loss of C_2H_2 and C_2H_6 as outlined in Gladstone et al. (1996). In the atmosphere of Jupiter, most of hydrocarbon compounds are synthesized in the regions above ~ 0.1 mbar (shown in the shaded area in Fig. 2). Below 0.1 mbar, the production of C_2H_2 through CH_4 photolysis mediated reactions is insufficient, because the process requires UV photons with wavelengths < 130 nm, which has been self-shielded by CH_4 . In this region, the photolysis of C_2H_6 (< 160 nm), which decreases strongly toward lower regions of the atmosphere, dominates the production of C_2H_2 . The major chemical loss of C_2H_2 and C_2H_6 is through hydrogenation and photolysis, respectively. As a consequence of this chemistry, C_2H_2 is close to being in photochemical steady-state in the regions below ~ 5 mbar altitude level and its vertical gradient is large in this altitude range. Above 5 mbar level, transport is important for C_2H_2 (Fig. 2). On the other hand, the abundance of C_2H_6 is controlled by transport and its vertical gradient is very small (see, e.g., Fig. 14 in Gladstone et al. 1996). Therefore, if meridional mixing is sufficiently rapid below the transition altitude to uniformly mix C_2H_6 with latitude, the tendency for uniform latitudinal mixing occurs also at 5 mbar. While above the transition altitude, uniform latitudinal mixing of C_2H_6 also results in uniform latitudinal mixing of C_2H_2 at 5 mbar.

Fig. 3 shows the 2-D distribution of C_2H_2 and C_2H_6 calculated with the reference model, in which $K_{yy} = 2 \times 10^{10}$ below 5 mbar level and $2 \times 10^9 \text{ cm}^2 \text{ s}^{-1}$ above. Additional observations at different levels in the atmosphere can help constrain the 2-D dynamical properties of the Jovian atmosphere.

vertical profiles of C_2H_2 and C_2H_6 at two latitudes. For comparison, 1-D results at low latitude are also overplotted. Additional observations at different levels in the atmosphere can help constrain the 2-D dynamical properties of the Jovian atmosphere.

In the above calculations whose results are summarized in Table 1, assumptions were made with respect to temperature and vertical eddy diffusion coefficients independent of latitudes and in the selection of chemistry reaction parameters. Several additional calculations were performed to assess the sensitivity of the derived values for K_{yy} with respect to these assumptions. In one sensitivity test, the temperature profile was progressively increased from 10° latitude so that, by 85° , the temperature profile was 10% larger. Table 1, model G, shows that, with the adjusted temperature distribution, the K_{yy} that best simulated the latitudinal variations in C_2H_2 and C_2H_6 in the Cassini observations is the same as derived above. This is consistent with the conclusions of Moses and Greathouse (2005) who found little sensitivity to temperature in their calculations. In a similar fashion, K_{zz} was modified linearly so that the value at 85° latitude was 10 times lower than the value at 10° latitude; enhanced K_{zz} at high latitudes cannot reproduce the measurements. The K_{yy} values that best simulated the Cassini observations (Table 1, model H) were again those derived earlier

in this paper. Finally, the same result for K_{yy} was found when the model chemistry was updated to be consistent with the reaction coefficients in Moses et al. (2005) (Table 1, model F). Therefore, the conclusions in this paper for the magnitude of meridional mixing as a function of altitude are robust with regard to reasonable selection of atmospheric temperature, vertical mixing, and chemistry.

4. Conclusion

Our model simulation results have two implications. First, the meridional transport time as short as 10 years ($K_{yy} \approx 10^{11} \text{ cm}^2 \text{ s}^{-1}$) exists only in the altitude range below the 10 mbar level. Second, above a transition level somewhere between 5 and 10 mbar, the meridional transport time is not shorter than ~ 1000 years ($K_{yy} \lesssim 10^9 \text{ cm}^2 \text{ s}^{-1}$). While these inferred K_{yy} values for the atmosphere at and below the 5-10 mbar level are consistent with the conclusions of Friedson et al. (1999) derived from an analysis of the SL9 debris evolution with time, the K_{yy} value above the transition level is much smaller than that ($\sim 10^{11} \text{ cm}^2 \text{ s}^{-1}$) derived from analysis of the time evolution of the distributions of gas-phase trace species deposited after the SL9 impact (Lellouch et al. 2002; Moreno et al. 2003; Griffith et al. 2004). There is no explanation at this time for this discrepancy.

It has been shown that CH_4 and C_2H_6 contribute to the heating and cooling of the stratosphere of Jupiter, respectively (Yelle et al. 2001). To a first order approximation, the cooling at/below 5 mbar level would be constant with latitude, being determined by two factors, the temperature and the abundance of C_2H_6 . These two are nearly constant between the equator and mid-latitudes (Flasar et al. 2004; Kunde et al. 2004, also Fig. 3). The heating function, however, is sensitive to the magnitude of the solar insolation and, consequently, it is a good approximation to assume that this function has the same latitude dependence as the solar insolation. Therefore, the global circulation could be driven by the differential heating between latitudes. This circulation driven by heating through absorption of radiation by gas-phase molecules will provide a first order estimate of the importance of aerosol heating in the stratosphere.

This research was supported in part by NASA grant NAG5-6263 to the California Institute of Technology. Special thank to Julie Moses for her insightful comments.

REFERENCES

- Conrath, B. J., P. J. Gierasch, and S. S. Leroy 1990. *Icarus* 83, 255-281.
- Flasar, F. M., Temporal behavior of Jupiters meteorology, in *Time-Variable Phenomena in the Jovian System*, M. J. S. Belton, R. A. West, and J. Rahe, eds., pp. 324V343, NASA SP-494, 1989.
- Flasar, F. M., and colleagues 2004. *Nature* 427, 132-135.
- Friedson, A. J., R. A. West, A. K. Hronek, N. A. Larsen, and N. Dalal 1999. *Icarus* 138, 141-156.
- Gierasch, P. J., B. J. Conrath, and J. A. Magalhaes 1986. *Icarus* 67, 456-483.
- Gladstone, G. R., M. Allen, and Y. L. Yung 1996. *Icarus* 119, 1-52.
- Griffith, C. A., B. Bezard, T. Greathouse, E. Lellouch, J. Lacy, D. Kelly, and M. J. Richter 2004. *Icarus* 170, 58-69.
- Kunde, V. G., and colleagues 2004. *Science* 305, 1582-1586.
- Lellouch, E., B. Bezard, J. I. Moses, G. R. Davis, P. Drossart, H. Feuchtgruber, E. A. Bergin, R. Moreno, and T. Encrenaz 2002. *Icarus* 159, 112-131.
- Moreno, R., A. Marten, H. E. Matthews, and Y. Biraud 2003. *Planetary and Space Science* 51, 591-611.
- Moses, J. I., B. Bezard, E. Lellouch, G. R. Gladstone, H. Feuchtgruber, and M. Allen 2000, *Icarus*, 143, 244-298.
- Moses, J. I., T. Fouchet, B. Bezard, G. R. Gladstone, E. Lellouch, and H. Feuchtgruber 2005, *J. Geophys. Res.* 110, E08001, doi:10.1029/2005JE002411.
- Moses, J. I., and T. K. Greathouse 2005, *J. Geophys. Res.*, 110, E09007, doi:10.1029/2005JE002450.
- Shia, R. L., Y. L. Ha, J. S. Wen, and Y. L. Yung 1990. *J. Geophys. Res.* 95, 7467-7483.
- West, R. A., A. J. Friedson, and J. F. Appleby 1992. *Icarus* 100, 245-259.
- Yelle, R. V., C. A. Griffith, and L. A. Young 2001. *Icarus* 152, 331-346.

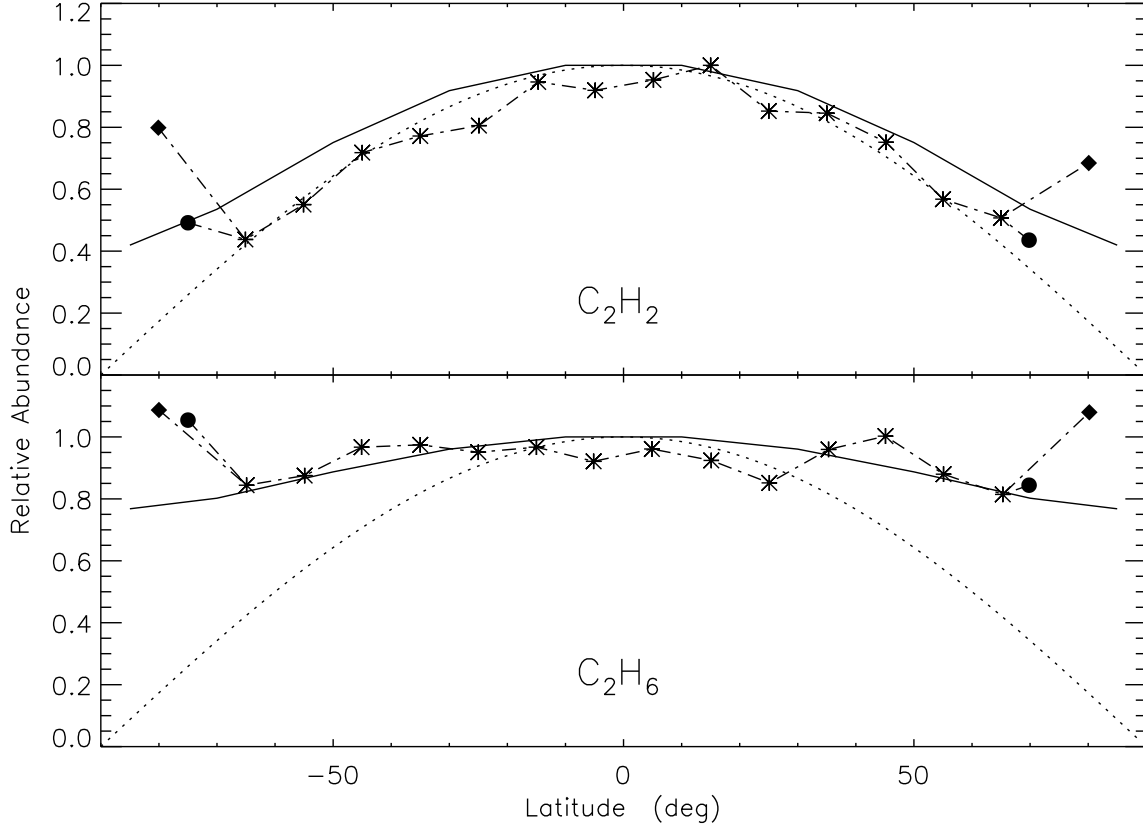


Fig. 1.— Relative abundances of C_2H_2 (upper) and C_2H_6 (lower) at 5 mbar as a function of latitude. Asterisks are the Cassini measurements (Kunde et al. 2004). Diamonds and circles are, respectively, high-latitude Cassini measurements that do include (diamonds) and do not include (circles) auroral longitudes. The calculated abundances of C_2H_2 and C_2H_6 are normalized to those at the equator. Solid line represents model results with the reference K_{yy} : constant $2 \times 10^{10} \text{ cm}^2 \text{ s}^{-1}$ below the 5 mbar altitude level and $2 \times 10^9 \text{ cm}^2 \text{ s}^{-1}$ above (model B). Dotted line represents the cosine function of latitude.

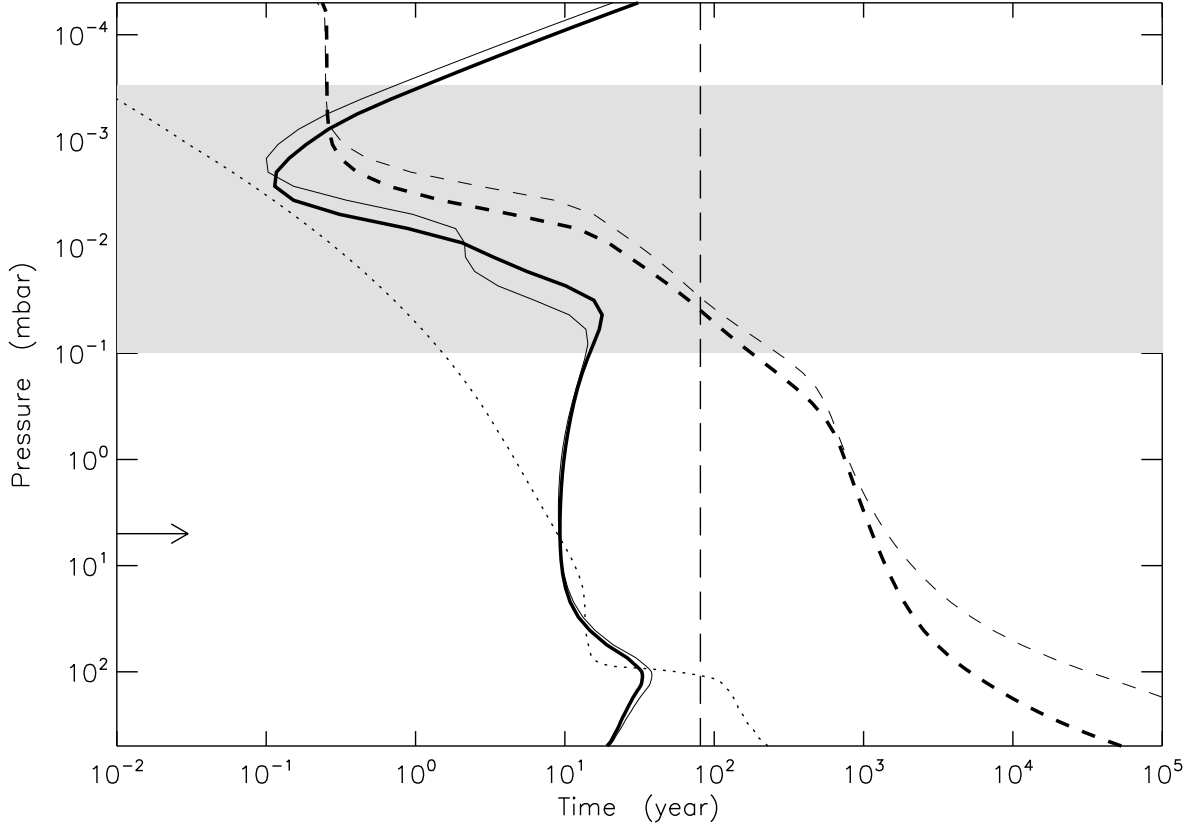


Fig. 2.— Timescales for the chemical loss of C_2H_2 (solid lines) and C_2H_6 (dashed lines) and for vertical transport (dotted line). The vertical transport timescale is defined by H^2/K_{zz} , where K_{zz} and H are the vertical diffusion coefficients of CH_4 and atmospheric scale height, respectively; values of time constants are derived from our reference model. Thick and thin lines represent values at latitudes 10° and 70° , respectively. The horizontal arrow indicates 5 mbar level where peak in the contribution function for the Cassini measurements of C_2H_2 and C_2H_6 lies. The vertical long-dashed line is a meridional mixing time equal to R_J^2/K_{yy} , where R_J is the radius of Jupiter and $K_{yy} = 2 \times 10^{10} \text{ cm}^2 \text{ s}^{-1}$. The shaded area shows the photochemical production region for the hydrocarbons.

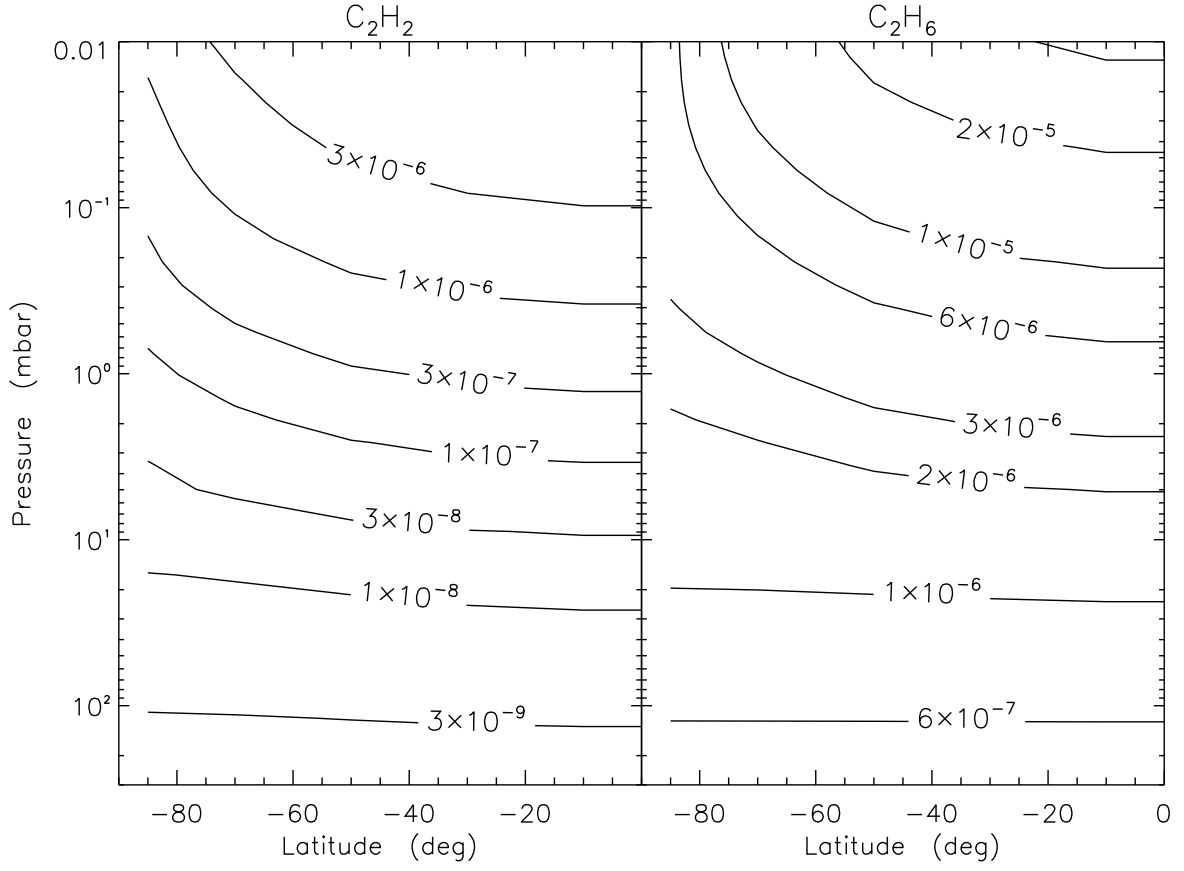


Fig. 3.— 2-D volume mixing ratio profiles of C_2H_2 (left) and C_2H_6 (right) calculated with the reference K_{yy} (model B).

Table 1. Summary of model results

| | Chemistry ^a | Temperature ^a | K_{zz} ^a | Transition ^b | K_{yy} below ^c | K_{yy} above ^c | C ₂ H ₂ ^d | C ₂ H ₆ ^d |
|------------|------------------------|--------------------------|-----------------------|-------------------------|-----------------------------|-----------------------------|--|--|
| Solar flux | ... | ... | ... | | | | 0.34 | 0.34 |
| Cassini | ... | ... | ... | | | | 0.50 | 0.87 |
| Model A | Standard | Standard | Standard | 5 | 2×10^{10} | 0 | 0.49 | 0.77 |
| Model B | Standard | Standard | Standard | 5 | 2×10^{10} | 2×10^9 | 0.54 | 0.80 |
| Model C | Standard | Standard | Standard | 10 | 2×10^{10} | 2×10^9 | 0.46 | 0.73 |
| Model D | Standard | Standard | Standard | 10 | 2×10^{11} | 0 | 0.46 | 0.75 |
| Model E | Standard | Standard | Standard | 10 | 2×10^{11} | 2×10^9 | 0.51 | 0.79 |
| Model F | Moses et al. (2005) | Standard | Standard | 5 | 2×10^{10} | 2×10^9 | 0.59 | 0.84 |
| Model G | Standard | $\times 1.1$ | Standard | 5 | 2×10^{10} | 2×10^9 | 0.49 | 0.76 |
| Model H | Standard | Standard | $\times 0.1$ | 10 | 2×10^{11} | 2×10^9 | 0.48 | 0.91 |

^a Standard chemistry is taken from Moses et al. (2000). Standard temperature and K_{zz} profiles are from Gladstone et al. (1996). Modified chemistry is from Moses et al. (2005). Reference temperature and K_{zz} profiles are set at equator (10°). The maximum changes in temperature (increase by 10%) and K_{zz} (reduced by a factor of 10) profiles are at 85° , with the change assumed to be linearly proportional to the angle of latitudes.

^b Transition level of K_{yy} profile. The level is given in units of mbar.

^c Values of K_{yy} below and above the transition level. K_{yy} is in units of $\text{cm}^2 \text{ s}^{-1}$.

^d Ratio of abundance at $\pm 70^\circ$ latitude to abundance at the equator. Values for Cassini measurements are averaged at $\pm 70^\circ$.